

LATENT DEGRADATION REPRESENTATION CONSTRAINT FOR SINGLE IMAGE DERAINING

Yuhong He^{*1}, Long Peng^{*2}, Lu Wang^{†1}, Jun Cheng³

Address - Line 1
Address - Line 2
Address - Line 3

ABSTRACT

Since rain shows a variety of shapes and directions, learning the degradation representation is extremely challenging for single image deraining. Existing methods mainly propose to designing complicated modules to implicitly learn latent degradation representation from rainy images. However, it is hard to decouple the content-independent degradation representation due to the lack of explicit constraint, resulting in over- or under-enhancement problems. To tackle this issue, we propose a novel Latent Degradation Representation Constraint Network (LDRCNet) that consists of the Direction-Aware Encoder (DAEncoder), Deraining Network, and Multi-Scale Interaction Block (MSIBlock). Specifically, the DAEncoder is proposed to extract latent degradation representation adaptively by first using the deformable convolutions to exploit the direction property of rain streaks. Next, a constraint loss is introduced to explicitly constraint the degradation representation learning during training. Last, we propose an MSIBlock to fuse with the learned degradation representation and decoder features of the deraining network for adaptive information interaction to remove various complicated rainy patterns and reconstruct image details. Experimental results on five synthetic and four real datasets demonstrate that our method achieves state-of-the-art performance. The source code is available at <https://github.com/Madeline-hyh/LDRCNet>.

Index Terms— Image Deraining, Representation Constraint, Deformable Convolution, Interactive Feature Fusion

1. INTRODUCTION

Images captured in rainy scenes will introduce artifacts like rain streaks and rain accumulation, which would lead to a loss of image detail and contrast. This will degrade the performance of outdoor computer vision systems, such as autonomous driving and video surveillance [1]. Therefore, restoring rainy images is an essential pre-processing step, and it has drawn much attention in recent years [2, 3, 4, 5, 6, 7]. However, single image deraining is still very challenging due to the difficulty in learning the degradation representation of rain streaks under various scenarios [8].

Traditional methods usually solve this problem by calculating a mathematical statistic to obtain diverse priors by exploring the physical properties of rain streaks [11, 12]. However, traditional methods have difficulty dealing with complex rainy images in real-world scenarios. Therefore, many deep learning-based methods have recently been proposed for single image deraining [13, 14, 15, 16, 17, 18]. For example, according to the direction property of rain streaks,

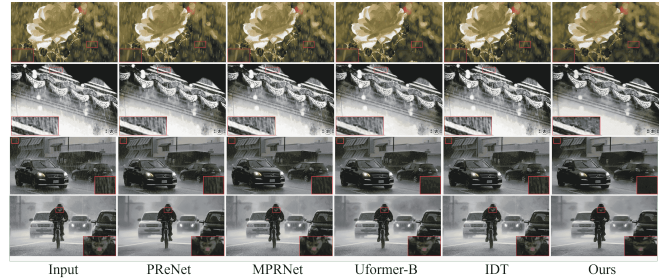


Fig. 1. Visual comparison on the real datasets, including Real15 [9] and Real300 [10]. Our method reconstructs credible textures with visually pleasing content.

Wang *et al.* [13] proposed a spatial attentive network to remove rain streaks in a local-to-global manner. Ma *et al.* [17] proposed to integrate degradation learning by an iterative framework. Albeit these methods have made significant progress, they still suffer from performance bottlenecks. This is because rain streaks and background are tightly coupled while existing methods focus on designing various modules to learn the degradation representation implicitly and are unable to decouple content-independent degradation representation, which would result in insufficient rain streak residual (*i.e.* under-enhancement) or smooth image textures (*i.e.* over-enhancement). Thus, explicit latent degradation representation learning is critical for single image deraining, which can handle spatially varying rainy patterns in different scenarios and adaptively enhance the structural information to decouple rainy images.

To achieve this goal, we propose a novel Latent Degradation Representation Constraint Network (LDRCNet) for explicit degradation learning to remove rain streaks and enhance image details adaptively. Specifically, we propose a direction-aware encoder (DAEncoder) to extract the latent degradation representation by first utilizing deformable convolution [19], which is based on the directional consistency of rain streaks in the local region [20] and the directional perception capacity of deformable convolution [21, 22]. To explicitly supervise the latent degradation representation, we introduce a constraint framework by utilizing the rain-free image and the latent degradation representation learned by the DAEncoder to reconstruct the corresponding rainy image during training. In this way, the latent degradation representation can disentangle the content-independent representation of rain degradation by optimizing the loss between the reconstructed result and the rainy image. To help the deraining network decouple the rain degradation and clean background, we propose a Multi-Scale Interaction Block (MSIBlock) to fuse the content-independent degradation representation and content-dependent decoder features of the deraining net-

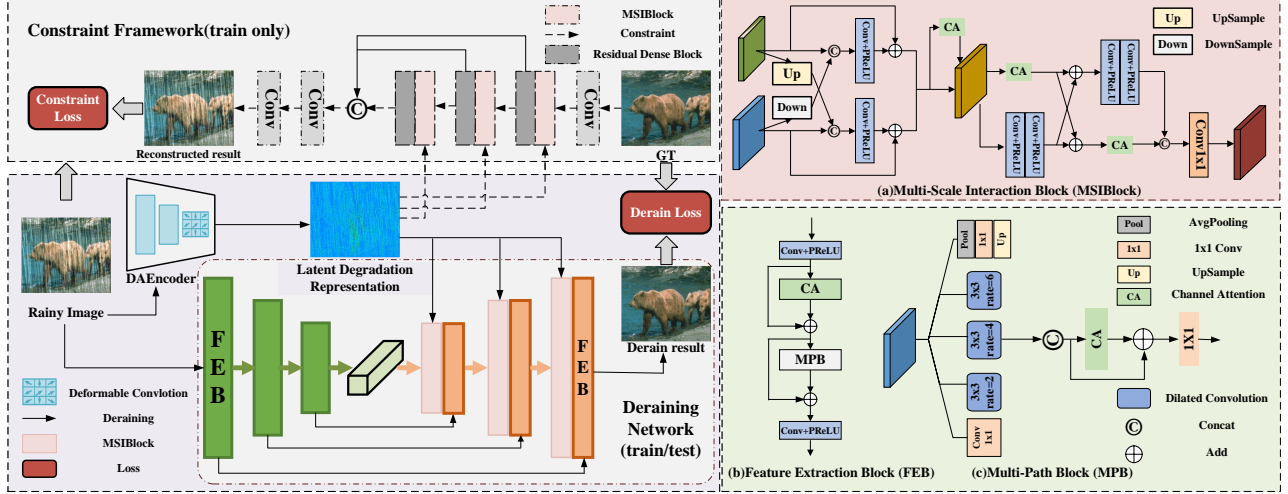


Fig. 2. Our proposed LDRCNet consists of the Direction-Aware Encoder (DAEncoder), Deraining Network, and Multi-Scale Interaction Block (MSIBlock). The constraint framework is proposed to provide explicit supervision to DAEncoder.

work. Such adaptive information interaction enables the deraining network to handle various and complicated rainy patterns effectively and reconstruct the details of images, and our deraining network only adopts a simple yet effective U-Net architecture without fancy design. The main contributions can be summarized as follows:

(1) We propose a novel Latent Degradation Representation Constraint Network (LDRCNet), which utilizes the Direction-Aware Encoder (DAEncoder) to learn the direction-aware degradation representation of rain streaks and is supervised by our proposed novel explicit constraint framework.

(2) We propose a novel Multi-Scale Feature Interaction Block (MSIBlock) that fuses learned degradation representation and decoder features of deraining networks to handle complex rain patterns and reconstruct image details adaptively.

(3) Experiments on five synthetic and four real-world datasets demonstrate that LDRCNet achieves state-of-the-art performance with explicit latent degradation representation constraints and adaptive information interaction.

2. PROPOSED METHOD

In this work, we propose a novel Latent Degradation Representation constraint Network (LDRCNet), as shown in Fig. 2. We design a Direction-Aware Encoder (DAEncoder) to perceive the directional properties of rain streaks and extract the latent degradation representation, and a constraint framework is proposed to provide explicit supervision. To effectively take advantage of the learned degradation representation for separating the rain layer and background, a Multi-Scale Feature Interaction Block (MSIBlock) is proposed for both the constraint framework and the deraining network.

2.1. Latent Degradation Representation Learning

Direction-Aware Encoder. Inspired by the observation of the direction consistency of rain streaks in local regions, we propose the DAEncoder that consists of several deformable convolutions [19] to learn multi-scale direction-aware degradation representation $deg = \{deg_1, deg_2, deg_3\}$ from the rainy image R . Specifically, deformable convolution can adjust the receptive field of the convolution kernel to adapt to the actual geometric variations of the rain streaks by using learnable offsets, which are used to extract the latent degradation representation of rain streaks with different shapes

and directions adaptively. For each location p_0 on the output feature map y , deformable convolution can be formulated as:

$$y(p_0) = \sum_{p_l \in L} w(p_l) \cdot x(p_0 + p_l + \Delta p_l) \quad (1)$$

where p_l enumerates the offset relative to the kernel center p_0 , which is in $L = \{(-1, -1), \dots, (1, 1)\}$. For example, L has nine choices for a 3×3 convolution kernel. w represents the weight of different locations. Compared with ordinary convolution, deformable convolution has an augmented offset Δp_l , which can be learned from the data to adapt to the different directions of rain streaks. Finally, the learning process of DAEncoder can be expressed as:

$$\{deg_1, deg_2, deg_3\} = E(R) \quad (2)$$

Constraint Framework. Most existing methods implicitly learn the degradation representation of rain streaks, which may result in insufficient rain residual or image textures being smoothed. To tackle this issue, we propose a constraint framework. Specifically, the framework learns to reconstruct the corresponding rainy image \hat{R} from the input of the rain-free image B and the multi-scale degradation representation. We introduce a constraint loss \mathcal{L}_C to optimize the loss between the reconstructed result and the original rainy image. In this way, the latent degradation representation learned by the DAEncoder can be supervised by the original rainy image R , which tends to be the content-independent representation of rain degradation. The constraint framework structure is based on several Residual Dense Blocks (RDB) [23] and MSIBlock, as shown in Fig. 2. The RDB can maximize the information flow and realize feature reuse. The MSIBlock is described in detail in Section 2.2.

The constraint framework C is only used in the training phase and the learning process and the loss function can be expressed as:

$$\mathcal{L}_C(R, \hat{R}) = \mathcal{L}(R, C(B, deg)) \quad (3)$$

2.2. Deraining with Learned Degradation Representation

To let the deraining network adaptively decouple rain streaks in complicated scenes and reconstruct the details of the images, we propose an MSIBlock to interact the learned content-independent degradation representation of rain streaks with the content-dependent decoder features of the deraining network for adaptive feature fusion.

Deraining Network. Rich multi-scale representation has fully

Table 1. Quantitative PSNR(\uparrow) and SSIM(\uparrow) comparisons with existing state-of-the-art deraining methods. Average means the average performance of the five benchmark datasets. The **bold** and underline represent the best and second-best performance.

Metrics	Test100		Rain100H		Rain100L		Test1200		Test2800		Average	
	PSNR	SSIM	PSNR	SSIM	PSNR	SSIM	PSNR	SSIM	PSNR	SSIM	PSNR	SSIM
DerainNet [24]	22.77	0.810	14.92	0.592	27.03	0.884	23.38	0.835	24.31	0.861	22.48	0.796
SEMI [25]	22.35	0.788	16.56	0.486	25.03	0.842	26.05	0.822	24.43	0.782	22.88	0.744
DIDMDN [26]	22.56	0.818	17.35	0.524	25.23	0.741	29.95	0.901	28.13	0.867	24.64	0.770
URML [27]	24.41	0.829	26.01	0.832	29.18	0.923	30.55	0.910	29.97	0.905	28.02	0.880
RESCAN [28]	25.00	0.835	26.36	0.786	29.80	0.881	30.51	0.882	31.29	0.904	28.59	0.858
SPANet [13]	23.17	0.833	26.54	0.843	32.20	0.951	31.36	0.912	30.05	0.922	28.66	0.892
PReNet [29]	24.81	0.851	26.77	0.858	32.44	0.950	31.36	0.911	31.75	0.916	29.43	0.897
MSPFN [30]	27.50	0.876	28.66	0.860	32.40	0.933	32.39	0.916	32.82	0.930	30.75	0.903
PCNet [31]	28.94	0.886	28.38	0.870	34.19	0.953	31.82	0.907	32.81	0.931	31.23	0.909
MPRNet [32]	<u>30.27</u>	0.897	<u>30.41</u>	0.890	36.40	0.965	32.91	0.916	<u>33.64</u>	<u>0.938</u>	<u>32.73</u>	0.921
IDLIR [17]	28.33	0.894	29.33	0.886	35.72	0.965	32.06	0.917	32.93	0.936	31.67	0.920
Uformer-B [16]	28.71	0.896	27.54	0.871	35.91	0.964	32.34	0.913	30.88	0.928	31.08	0.914
IDT [33]	29.69	<u>0.905</u>	29.95	0.898	37.01	0.971	31.38	0.908	33.38	0.937	32.28	<u>0.924</u>
Semi-SwinDerain [34]	28.54	0.893	28.79	0.861	34.71	0.957	30.96	0.909	32.68	0.932	31.14	0.910
DAWN [35]	29.86	0.902	29.89	0.889	35.97	0.963	32.76	0.919	-	-	32.12	0.918
LDRCNet(Ours)	31.17	0.914	30.63	<u>0.897</u>	<u>36.83</u>	<u>0.968</u>	<u>32.89</u>	<u>0.917</u>	33.74	0.940	33.05	0.927

Table 2. Quantitative NIQE(\downarrow)/BRISQUE(\downarrow) performance comparisons on the real-world datasets.

Datasets	UMRL [27]	PReNet [29]	MSPFN [30]	PCNet [31]	MPRNet [32]	Uformer-B [16]	IDT [33]	LDRCNet(Ours)
Real15 [9]	16.60/24.09	16.04/25.29	17.03/23.60	16.19/25.61	16.48/23.92	15.71/ 18.67	15.60/28.35	14.60 /18.68
Real300 [10]	15.78/26.39	15.12/23.57	15.34/28.27	15.47/28.99	15.08/28.69	14.90/24.35	15.45/ 23.48	14.67 /28.93
RID [36]	12.19/40.67	12.45/38.89	11.74/41.88	12.03/40.76	11.79/44.04	11.54/36.38	12.49/ 35.99	11.49 /37.79
RIS [36]	16.30/47.98	16.74/48.83	15.73 /47.45	16.19/49.00	16.88/52.11	16.00/ 45.06	17.45/49.86	15.76/49.08

demonstrated its effectiveness in removing rain streaks [30]. Therefore, we use a simple yet effective U-Net architecture as the deraining network to extract feature maps at different scales. To retrieve more contextual information, we further propose a Multi-Path Block (MPB) in each feature extraction layer to aggregate more features of rain streaks with a larger receptive field. The MPB has several branches to enlarge the receptive field in parallel, as shown in Fig. 2 (c). In particular, the MPB first utilizes 1×1 convolution, avgpooling, and dilated convolutions with different dilation rates to capture the multi-scale structure of rain streaks while maintaining negligible parameter increase. Then, all of the feature maps are concatenated, and Channel Attention (CA) is used to adaptively focus on the important feature information. Last, the convolution is used to output the final result \hat{B} . The decoder structure is the same as the encoder, and the learned content-independent degradation representation is embedded in the decoder feature by MSIBlock.

After obtaining the pre-trained DAEncoder E , we freeze it and retrain the deraining network D , which can be expressed as:

$$\mathcal{L}_D(B, \hat{B}) = \mathcal{L}(B, D(R, deg)) \quad (4)$$

where R and B denote the input of the original rainy image and its corresponding clean image.

Multi-Scale Interaction Block. To make full use of the multi-scale degradation representation learned by DAEncoder to enhance the structural details and decouple the rain streaks, we propose to embed latent degradation representation into the deraining network. One simple solution is concatenation, but such an operation cannot effectively exploit learned degradation representation to extract complicated rain streaks and may cause optimization interference. Therefore, we propose the MSIBlock for adaptive information interaction. Specifically, we first utilize convolutions to align the content-independent degradation representation deg and content-dependent decoder features \mathcal{F}_r of the deraining network, and then Channel Attention (Att) is used to adaptively enhance the important interactive

information, as shown in Fig. 2 (a). Last, diverse combinations of Residual Blocks (RB) can further reconstruct the detail of the image. The MSIBlock can be denoted as:

$$\begin{aligned} \mathcal{F}_c &= \text{Att}(\text{Concat}(\text{Conv}(\mathcal{F}_r), \text{Conv}(deg))) \\ \hat{\mathcal{F}} &= \text{Concat}(\text{RB}(\mathcal{F}_c)) \end{aligned} \quad (5)$$

where \mathcal{F}_c and $\hat{\mathcal{F}}$ denotes the concatenated and the output feature. The MSIBlock is also used in the constraint framework for feature fusion.

2.3. Loss Function

The total training loss $\mathcal{L}_{\text{total}}$ can be formulated as follows:

$$\mathcal{L}_{\text{total}} = \lambda_1 \mathcal{L}_D(B, \hat{B}) + \lambda_2 \mathcal{L}_C(R, \hat{R}) \quad (6)$$

where λ_1 and λ_2 denote the balancing parameters. Following previous work [26, 30, 37, 14], we use widely-used MSELoss as \mathcal{L} .

3. EXPERIMENTS

3.1. Implementation Details

In our experiment, we set the training patch size to 256×256 and set λ_1 and λ_2 to 1 and 1. We use the Adam optimizer with an initial learning rate 3×10^{-4} for training our methods on four NVIDIA GeForce RTX 3090 GPUs at Pytorch. And the learning rate of Adam is steadily decreased to 1×10^{-6} using the cosine annealing strategy.

3.2. Datasets and Compared Methods

Following [30, 32], we conduct experiments on the Rain13k dataset, which contains 13,712 images with rain streaks of various scales and directions for training, and Test100 [38], Rain100H [9], Rain100L [9], Test1200 [26] and Test2800 [24] are used as test data. Real datasets are also considered to test the generalization, including Real15 [9], Real300 [10], Rain in Driving (RID), and Rain in Surveillance (RIS) [36]. RID and RIS have a total of 2495 and 2348

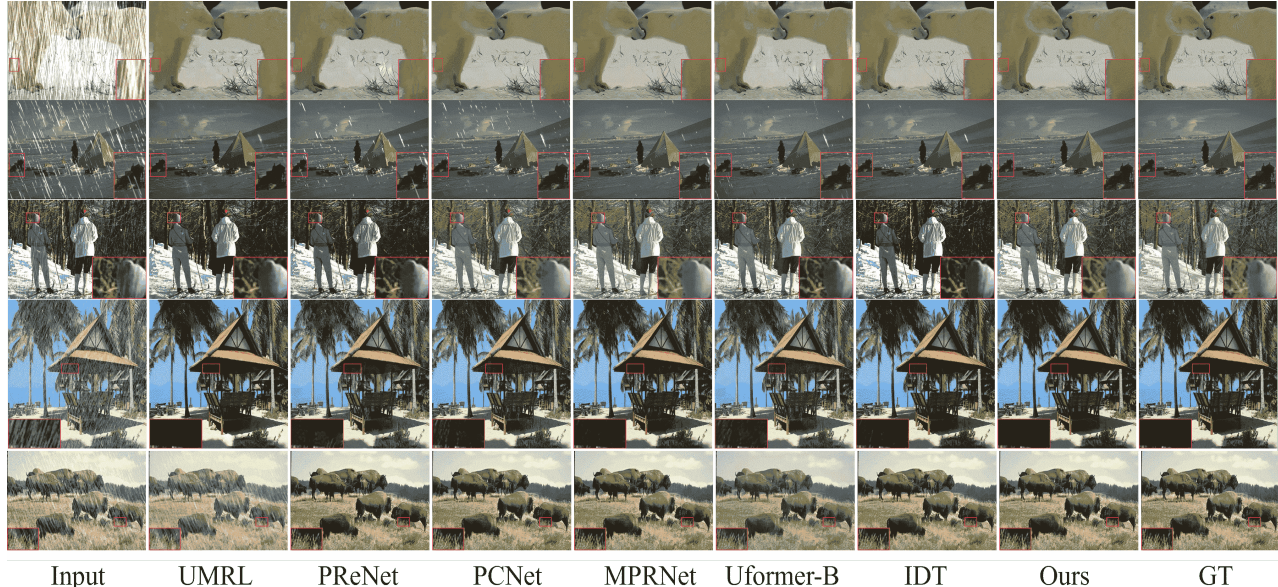


Fig. 3. Visual comparison on the Rain100H [9], Rain100L [9], Test100 [38], Test1200 [26], and Test2800 [24] datasets.

Table 3. Ablation studies on different settings.

	S1	S2	S3	S4	S5	Ours
PSNR	27.52	28.37	29.43	29.89	29.96	30.60
SSIM	0.847	0.865	0.873	0.879	0.878	0.897

images in real scenes, respectively. We compare our method with the existing fifteen state-of-the-art deraining methods. Continuing along the trajectory of previous works [33, 32, 29], we use PSNR and SSIM to evaluate the deraining performance of synthetic images, and utilize NIQE and BRISQUE to evaluate the real dataset.

3.3. Quantitative and Qualitative Experiment

Synthetic Scene. To quantitatively demonstrate the superiority of our method, we compare our method with several existing SOTA methods, and the results are shown in Tab. 1. Our method achieves the best results on the average performance of five test datasets and we also perform visual comparisons, as shown in Fig. 3. Compared with existing methods, we can observe that our method removes rain streaks more completely and restores better texture details of the background, while other approaches retain some obvious rain streaks or lose important details of the background.

Real Scene. We further conduct experiments on four real-world datasets: Real15 [9], Real300 [10], RID [36], and RIS [36]. Quantitative results of NIQE and BRISQUE are shown in Tab. 2. Our LDR-CNet achieves the best NIQE performance on Real15, Real300, and RID datasets, which demonstrates that our method achieves good robustness and generalization in real-world scenarios. Visual comparisons on Real15 and Real300 are illustrated in Fig. 1.

3.4. Feature Visualization

To verify the effectiveness of our network structure, we visualize the intermediate feature, as shown in Fig. 4. The latent degradation representation with explicit constraints learned content-independent rain degradation, which helps to remove rain streaks. On the contrary, the deraining network learned content-dependent features, which helps to reconstruct the details.

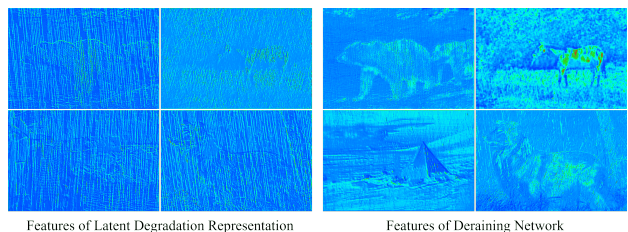


Fig. 4. Visualization of the latent feature.

3.5. Ablation Studies

We perform ablation studies on the Rain100H: S1: Without deraining network, and we use convolutions to map the latent degradation representation to rain residual; S2: Without the DAEncoder and the constraint framework; S3: Without constraint framework; S4: Using vanilla convolution to replace the deformable convolution; S5: Using concatenation to replace the MSIBlock. In Tab. 3, we can observe that all components are crucial for our LDR-CNet. For example, the performance of the proposed method degrades 1.17dB and 0.019 on PSNR and SSIM without the constraint, demonstrating the superiority of our constraint strategy. The performance degrades 0.71dB and 0.018 on PSNR and SSIM without the deformable convolution, demonstrating that direction-aware information is helpful for decoupling rainy patterns effectively. The performance degrades 0.64dB and 0.019 without the MSIBlock, demonstrating that adaptive information interaction is critical to removing rainy patterns.

4. CONCLUSION

In this paper, we propose a novel LDR-CNet for explicit degradation learning to remove rain and reconstruct details adaptively. Specifically, we propose a DAEncoder to utilize the directional properties of rain streaks and a constraint network to provide an explicit guide. To make the well-learned latent degradation representation contribute to the deraining network, we propose the MSIBlock for adaptive information interaction, which helps to remove spatially varying rain patterns adaptively. The proposed network is evaluated on five synthetic and four real prevailing datasets, demonstrating it has state-of-the-art performance compared with several representative methods.

5. REFERENCES

- [1] Chen Zhang, Zefan Huang, Beatrix Xue Lin Tung, Marcelo H Ang, and Daniela Rus, “Smartrainnet: Uncertainty estimation for laser measurement in rain,” in *ICRA*. IEEE, 2023, pp. 10567–10573.
- [2] Long Peng, Aiwen Jiang, Haoran Wei, Bo Liu, and Mingwen Wang, “Ensemble single image deraining network via progressive structural boosting constraints,” *Signal Processing: Image Communication*, vol. 99, pp. 116460, 2021.
- [3] Yuntong Ye, Yi Chang, Hanyu Zhou, and Luxin Yan, “Closing the loop: Joint rain generation and removal via disentangled image translation,” in *CVPR*, 2021, pp. 2053–2062.
- [4] Qiaosi Yi, Juncheng Li, Qinyan Dai, Faming Fang, Guixu Zhang, and Tiejong Zeng, “Structure-preserving deraining with residue channel prior guidance,” in *ICCV*, 2021, pp. 4238–4247.
- [5] Yang Wang, Long Peng, Liang Li, Yang Cao, and Zheng-Jun Zha, “Decoupling-and-aggregating for image exposure correction,” in *CVPR*, 2023, pp. 18115–18124.
- [6] Yawei Li, Yulun Zhang, Radu Timofte, Luc Van Gool, Lei Yu, Youwei Li, Xinpeng Li, Ting Jiang, Qi Wu, Mingyan Han, et al., “Ntire 2023 challenge on efficient super-resolution: Methods and results,” in *Proceedings of the IEEE/CVF Conference on Computer Vision and Pattern Recognition*, 2023, pp. 1921–1959.
- [7] Qiu Hai Yan, Aiwen Jiang, Kang Chen, Long Peng, Qiaosi Yi, and Chunjie Zhang, “Textual prompt guided image restoration,” *arXiv preprint arXiv:2312.06162*, 2023.
- [8] Siyuan Li, Iago Breno Araujo, Wenqi Ren, Zhangyang Wang, Eric K Tokuda, Roberto Hirata Junior, Roberto Cesar-Junior, Jiawan Zhang, Xiaojie Guo, and Xiaochun Cao, “Single image deraining: A comprehensive benchmark analysis,” in *CVPR*, 2019, pp. 3838–3847.
- [9] Wenhan Yang, Robby T Tan, Jiashi Feng, Jiaying Liu, Zongming Guo, and Shuicheng Yan, “Deep joint rain detection and removal from a single image,” in *CVPR*, 2017, pp. 1357–1366.
- [10] Xueyang Fu, Borong Liang, Yue Huang, Xinghao Ding, and John Paisley, “Lightweight pyramid networks for image deraining,” *TNNLS*, vol. 31, no. 6, pp. 1794–1807, 2019.
- [11] Yu Li, Robby T Tan, Xiaojie Guo, Jiangbo Lu, and Michael S Brown, “Rain streak removal using layer priors,” in *CVPR*, 2016, pp. 2736–2744.
- [12] Lei Zhu, Chi-Wing Fu, Dani Lischinski, and Pheng-Ann Heng, “Joint bi-layer optimization for single-image rain streak removal,” in *ICCV*, 2017, pp. 2526–2534.
- [13] Tianyu Wang, Xin Yang, Ke Xu, Shaozhe Chen, Qiang Zhang, and Rynson W.H. Lau, “Spatial attentive single-image deraining with a high quality real rain dataset,” in *CVPR*, 2019, pp. 12262–12271.
- [14] Long Peng, Aiwen Jiang, Qiaosi Yi, and Mingwen Wang, “Cumulative rain density sensing network for single image derain,” *SPL*, vol. 27, pp. 406–410, 2020.
- [15] Yuhong He, Tao Zeng, Ye Xiong, Jialu Li, and Haoran Wei, “Deep leaning based frequency-aware single image deraining by extracting knowledge from rain and background,” *MLKE*, vol. 4, no. 3, pp. 738–752, 2022.
- [16] Zhendong Wang, Xiaodong Cun, Jianmin Bao, Wengang Zhou, Jianzhuang Liu, and Houqiang Li, “Uformer: A general u-shaped transformer for image restoration,” in *CVPR*, 2022, pp. 17683–17693.
- [17] Mingyu Ma, Dongwei Ren, and Yajun Yang, “Integrating degradation learning into image restoration,” in *ICME*. IEEE, 2022, pp. 1–6.
- [18] Zhifeng Wang, Aiwen Jiang, Chunjie Zhang, Hanxi Li, and Bo Liu, “Self-supervised multi-scale pyramid fusion networks for realistic bokeh effect rendering,” *Journal of Visual Communication and Image Representation*, vol. 87, pp. 103580, 2022.
- [19] Jifeng Dai, Haozhi Qi, Yuwen Xiong, Yi Li, Guodong Zhang, Han Hu, and Yichen Wei, “Deformable convolutional networks,” in *ICCV*, 2017, pp. 764–773.
- [20] Yang Liu, Ziyu Yue, Jinshan Pan, and Zhixun Su, “Unpaired learning for deep image deraining with rain direction regularizer,” in *ICCV*, October 2021, pp. 4753–4761.
- [21] Ashutosh Kulkarni and Subrahmanyam Murala, “Aerial image dehazing with attentive deformable transformers,” in *WACV*, January 2023, pp. 6305–6314.
- [22] Juntao Guan, Rui Lai, Yang Lu, Yangang Li, Huanan Li, Lichen Feng, Yintang Yang, and Lin Gu, “Memory-efficient deformable convolution based joint denoising and demosaicing for uhd images,” *TCSVT*, vol. 32, no. 11, pp. 7346–7358, 2022.
- [23] Yulun Zhang, Yapeng Tian, Yu Kong, Bineng Zhong, and Yun Fu, “Residual dense network for image super-resolution,” in *CVPR*, 2018, pp. 2472–2481.
- [24] Xueyang Fu, Jiabin Huang, Delu Zeng, Yue Huang, Xinghao Ding, and John Paisley, “Removing rain from single images via a deep detail network,” in *CVPR*, 2017, pp. 3855–3863.
- [25] Wei Wei, Deyu Meng, Qian Zhao, Zongben Xu, and Ying Wu, “Semi-supervised transfer learning for image rain removal,” in *CVPR*, 2019, pp. 3877–3886.
- [26] He Zhang and Vishal M Patel, “Density-aware single image deraining using a multi-stream dense network,” in *CVPR*, 2018, pp. 695–704.
- [27] Rajeev Yasarla and Vishal M Patel, “Uncertainty guided multi-scale residual learning-using a cycle spinning cnn for single image de-raining,” in *CVPR*, 2019, pp. 8405–8414.
- [28] Xia Li, Jianlong Wu, Zhouchen Lin, Hong Liu, and Hongbin Zha, “Recurrent squeeze-and-excitation context aggregation net for single image deraining,” in *ECCV*, 2018, pp. 254–269.
- [29] Dongwei Ren, Wangmeng Zuo, Qinghua Hu, Pengfei Zhu, and Deyu Meng, “Progressive image deraining networks: A better and simpler baseline,” in *CVPR*, 2019, pp. 3937–3946.
- [30] Kui Jiang, Zhongyuan Wang, Peng Yi, Chen Chen, Baojin Huang, Yimin Luo, Jiayi Ma, and Junjun Jiang, “Multi-scale progressive fusion network for single image deraining,” in *CVPR*, 2020, pp. 8346–8355.
- [31] Kui Jiang, Zhongyuan Wang, Peng Yi, Chen Chen, Zheng Wang, Xiao Wang, Junjun Jiang, and Chia-Wen Lin, “Rain-free and residue hand-in-hand: A progressive coupled network for real-time image deraining,” *TIP*, vol. 30, pp. 7404–7418, 2021.
- [32] Syed Waqas Zamir, Aditya Arora, Salman Khan, Munawar Hayat, Fahad Shahbaz Khan, Ming-Hsuan Yang, and Ling Shao, “Multi-stage progressive image restoration,” in *CVPR*, 2021, pp. 14821–14831.
- [33] Jie Xiao, Xueyang Fu, Aiping Liu, Feng Wu, and Zheng-Jun Zha, “Image de-raining transformer,” *TPAMI*, 2022.
- [34] Chun Ren, Danfeng Yan, Yuanqiang Cai, and Yangchun Li, “Semi-swinderain: Semi-supervised image deraining network using swin transformer,” in *ICASSP*. IEEE, 2023, pp. 1–5.
- [35] Kui Jiang, Wenxuan Liu, Zheng Wang, Xian Zhong, Junjun Jiang, and Chia-Wen Lin, “Dawn: Direction-aware attention

wavelet network for image deraining,” in *ACM MM*, 2023, pp. 7065–7074.

- [36] Siyuan Li, Wenqi Ren, Jiawan Zhang, Jinke Yu, and Xiaojie Guo, “Single image rain removal via a deep decomposition–composition network,” *CVIU*, vol. 186, pp. 48–57, 2019.
- [37] Zhifeng Wang and Aiwen Jiang, “A dense prediction vit network for single image bokeh rendering,” in *PRCV*. Springer, 2022, pp. 213–222.
- [38] He Zhang, Vishwanath Sindagi, and Vishal M Patel, “Image de-raining using a conditional generative adversarial network,” *TCSVT*, vol. 30, no. 11, pp. 3943–3956, 2019.